Metal Exchange Method Using Au 25 Nanoclusters as Templates for Alloy Nanoclusters with Atomic Precision

ARTICLE *in* JOURNAL OF THE AMERICAN CHEMICAL SOCIETY · MARCH 2015

Impact Factor: 12.11 · DOI: 10.1021/ja511635g · Source: PubMed

10 AUTHORS, INCLUDING:

Shuxin Wang
Anhui University
34 PUBLICATIONS **359** CITATIONS
SEE PROFILE

Shan Jin
Anhui University
9 PUBLICATIONS **26** CITATIONS
SEE PROFILE

Jun Zhang
Anhui Jianzhu University
39 PUBLICATIONS **166** CITATIONS
SEE PROFILE

Peng li
Anhui University
64 PUBLICATIONS **914** CITATIONS
SEE PROFILE

JACS
JOURNAL OF THE AMERICAN CHEMICAL SOCIETY

Communication

pubs.acs.org/JACS

Metal Exchange Method Using Au_{25} Nanoclusters as Templates for Alloy Nanoclusters with Atomic Precision

Shuxin Wang,[†,§] Yongbo Song,[†,§] Shan Jin,[†] Xia Liu,[‡] Jun Zhang,[†] Yong Pei,[‡] Xiangming Meng,[†] Man Chen,[†] Peng Li,[†] and Manzhou Zhu*[,†]

[†]Department of Chemistry and Center for Atomic Engineering of Advanced Materials, Anhui University, Hefei, Anhui 230601, People's Republic of China

[‡]Department of Chemistry, Key Laboratory of Environmentally Friendly Chemistry and Applications of Ministry of Education, Xiangtan University, Xiangtan, Hunan 411105, People's Republic of China

Supporting Information

ABSTRACT: A metal exchange method based upon atomically precise gold nanoclusters (NCs) as templates is devised to obtain alloy NCs including $Cu_xAu_{25-x}(SR)_{18}$, $Ag_xAu_{25-x}(SR)_{18}$, $Cd_1Au_{24}(SR)_{18}$, and $Hg_1Au_{24}(SR)_{18}$ via reaction of the template with metal thiolate complexes of Cu^{II}, Ag^{I}, Cd^{II}, and Hg^{II} (as opposed to common salt precursors such as $CuCl_2$, $AgNO_3$, etc.). Experimental results imply that the exchange between gold atoms in NCs and those of the second metal in the thiolated complex does not necessarily follow the order of metal activity (i.e., galvanic sequence). In addition, the crystal structure of the exchange product ($Cd_1Au_{24}(SR)_{18}$) is successfully determined, indicating that the Cd is in the center of the 13-atom icosahedral core. This metal exchange method is expected to become a versatile new approach for synthesizing alloy NCs that contain both high- and low-activity metal atoms.

Precisely doped metal nanoclusters (NCs) with a few tens of metal atoms have emerged as a new class of nanomaterial.[1] These small, doped NCs are attracting wide interest owing to their synergistic properties that depend on the atomic composition, such as catalytic activity, which is largely enhanced for single Pd- or Pt-atom-doped M_1Au_{24} NCs (M = Pd/Pt) compared to the homo-gold counterpart,[2] as well as luminescence, which becomes stronger in Ag- or Cu-doped gold NCs.[3] Controlling the number of each type of metal atoms and their doping sites in the alloy (or bimetallic) NC is crucial, as the metal composition and doping sites are the keys to tailoring the alloy NC's properties. Controlled synthesis of doped NCs at the atomic level is still quite challenging, and until now only a few doped NCs have been attained with atomic precision and molecular purity.[2,4,5] A conventional synthetic strategy involves reducing a mixture of metal precursors by $NaBH_4$ in the presence of ligands, such as the cases of $M_xAu_{25-x}(SR)_{18}$ (M = Ag or Cu) NCs.[4] To effectively produce alloy NCs, new methods should be devised for synthesizing alloy NCs with designed metal compositions, precise atom numbers, and metal doping site control. Several fundamental questions remain about metal doping:[3c] What metals can be doped into Au NCs? Can one precisely control the number of doping atoms? Where would these dopants go in the Au NC structure?

Recent research has reported an anti-galvanic reduction (AGR) approach, suggesting that when Au/Ag nanoparticle size is smaller than ~3 nm (i.e., in the NC regime), their reducing capability is enhanced;[6] for example, Au NCs can reduce Ag^+ and Cu^{2+}, which are more active in bulk metals than Au, and similarly Ag NCs can reduce Cu^{2+}.[6a] The order of metal activity was summarized as Fe > Ni > [Au NCs] > Cu > Ag.[6a] These results suggest that the AGR method can only be applied to synthesize CuAu and AgAu NCs; therefore, the production of doped NCs is quite limited, especially alloy NCs with the second metal having high activity, which is particularly attractive for tuning catalytic, magnetic, and other properties.[2,7]

Previous theoretical work indicates that the stability of $M_xAu_{25-x}(SR)_{18}$ (X = Pd, Ag, and Cd) NCs should be similar to that of $Au_{25}(SR)_{18}^-$.[8,9c] The stability of these clusters is in part due to their $8e^-$ shell closing structure.[8,9] This electronic factor indicates that, in the AGR process, Ag and Cu doping should meet the $8e^-$ shell closing. If this is true, metal doping may not exclusively follow the order of metal activity, since Cd is a high-activity metal in the series (Fe > Cd > Co > Ni > Pb > [Au NCs] > Cu > Hg > Ag > Pd > Pt > Au), and Cd ($5s^2$) might be doped into the $Au_{25}(SR)_{18}^-$ NC to form $Cd_1Au_{24}(SR)_{18}^0$. Consideration of the electronic factor over the metal activity offers a new perspective for synthetic control of alloy NCs, especially for doping high-activity metal into Au NCs, which is not feasible via the AGR method.

This work demonstrates a metal exchange method for obtaining alloy NCs using $Au_{25}(SR)_{18}^-$ NCs as the template. Reaction of the template with a series of metal−thiolate complexes (as opposed to metal salts) of groups 10−12 gives rise to Ag_xAu_{25-x}, Cu_xAu_{25-x}, Cd_1Au_{24}, and Hg_1Au_{24}, while Ni_xAu_{25-x}, Pd_xAu_{25-x}, and Pt_xAu_{25-x} are not formed. This distinctly different behavior between group 10 and groups 11−12 metals offers some important implications for the metal exchange mechanism. The crystal structure of Cd_1Au_{24} not only shows that the charge of this cluster is neutral but also indicates that the Cd atom is in the center of the M_{13} core; in other words, this Cd atom is in the metallic form.

In a typical experiment, the $Au_{25}(SR)_{18}^-$ NC (Supporting Information (SI), Figure S1) reacted with thiolated metal

Received: November 12, 2014

DOI: 10.1021/ja511635g
J. Am. Chem. Soc. XXXX, XXX, XXX−XXX

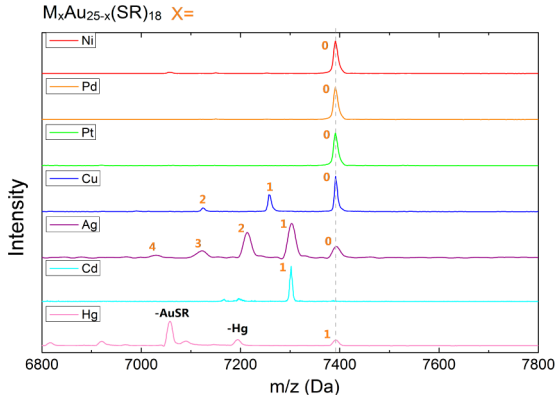

Figure 1. MALDI-MS of $M_xAu_{25-x}(SR)_{18}$ (x as indicated in each spectrum) after reaction with different metal ions (Ni^{II}, Pd^{II}, Pt^{II}, Cu^{II}, Ag^{I}, Cd^{II}, and Hg^{II}, all in thiolate complexes). R = C_2H_4Ph. The reaction time was set to 2 h. See Figure S3 for wider range mass spectra (2000–20000 range).

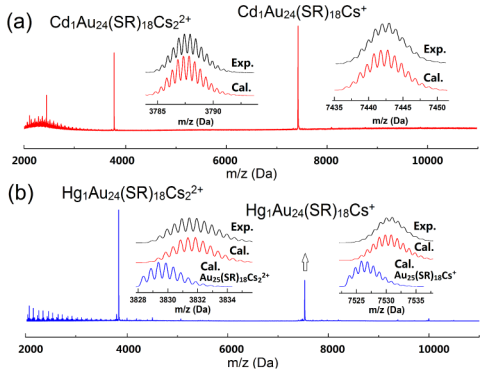

Figure 2. (a) ESI mass spectrum of $Cd_1Au_{24}(SC_2H_4Ph)_{18}$ NCs. Insets are experimental and simulated isotope patterns of $Cd_1Au_{24}(SC_2H_4Ph)_{18}Cs_2^{2+}$ and $Cd_1Au_{24}(SC_2H_4Ph)_{18}Cs^+$, respectively. (b) ESI-MS spectrum of $Hg_1Au_{24}(PhC_2H_4S)_{18}$ NCs. Insets are experimental and simulated isotope patterns of $Hg_1Au_{24}(SC_2H_4Ph)_{18}Cs_2^{2+}$ (together with simulated $Au_{25}(SC_2H_4Ph)_{18}Cs_2^{2+}$) and $Hg_1Au_{24}(SC_2H_4Ph)_{18}Cs^+$ (together with simulated $Au_{25}(SC_2H_4Ph)_{18}Cs^+$), respectively.

complexes including $Ag^{I}SR$, $Cu^{II}(SR)_2$, $Cd^{II}(SR)_2$, $Hg^{II}(SR)_2$, $Ni^{II}(SR)_2$, $Pd^{II}(SR)_2$, and $Pt^{II}(SR)_2$, where R = C_2H_4Ph hereafter. We note that $Zn^{II}(SR)_2$ could not be synthesized, as thiol cannot react with Zn^{2+}. Matrix-assisted laser desorption/ionization mass spectrometry (MALDI-MS) and UV/vis spectroscopy were used to monitor whether the metal exchange process occurred. As shown in Figure 1, Ni-, Pd-, and Pt-doped Au_{25} NCs were not detected in MALDI-MS. The Cu/Au (or Ag/Au) alloy NCs showed a distribution of peaks corresponding to different numbers of Ag (or Cu) atoms doped into the 25-atom cluster (Figures 1 and S2), and the mass difference between peaks was equal to the Au and Ag (or Cu) atomic mass difference (i.e., $M_{Au} - M_{Cu}$ = 133.5 Da, $M_{Au} - M_{Ag}$ = 89 Da). The total number of metal atoms is, however, preserved at 25 in all NCs, implying the robustness of the 25-atom structure. The Cu/Ag doping results are consistent with the previously reported AGR, in which Au NCs could reduce Cu^{2+} and Ag^+ ions, albeit Cu and Ag are more active than Au in the form of bulk metals.

Surprisingly, Au_{25} NCs were not able to reduce $Ni^{II}/Pd^{II}/Pt^{II}$, but they reacted readily with Cd^{II} (note: Cd metal is more active than Ni, Pd, and Pt), and the Cd-doping product was identified to be mono-doped $Cd_1Au_{24}(SR)_{18}$ (m/z = 7309, Figure 1). No residual $Au_{25}(SR)_{18}$ was observed in the mass spectrum, indicating a nearly complete conversion. These findings are important because Pt and Pd are less active than Ag and Cu, while Cd is more active than Ni and would not be doped into Au NCs according to the AGR approach. But our results suggest that $Au_{25}(SR)_{18}^-$ is capable of reacting with Cd^{II}. For mercury doping, a single Hg atom was doped into the Au NC (Figure 1) in nearly 100% yield; of note, the Hg and Au masses are very close, and thus the mass peak of $Hg_1Au_{24}(SR)_{18}$ appears at the $Au_{25}(SR)_{18}$ position (Figure 1), but high-precision MS analysis rules out $Au_{25}(SR)_{18}$ (vide infra).

Ag/Cu/Cd/Hg doping into the 25-atom NC perturbs the optical absorption (Figure S4), but the spectral profile is essentially retained in these cases, while when metal salts were used, the NCs finally decomposed (Figure S5). To confirm the newly attained single-Cd/Hg-doped $M_1Au_{24}(SR)_{18}$ NCs and probe their charge states, we further performed electrospray ionization (ESI) MS analysis. For $Cd_1Au_{24}(SR)_{18}$ NCs, the positive mode ESI spectrum (Figure 2a) showed two intense peaks at m/z 3787.9 and 7442.9 (the most abundant isotope peaks); since cesium acetate was added to form Cs^+ adducts, these peaks are assigned to $Cd_1Au_{24}(SR)_{18}Cs_2^{2+}$ (calcd m/z 3787.8) and $Cd_1Au_{24}(SR)_{18}Cs^+$ (calcd m/z 7442.8), respectively, and the experimental and simulated isotope patterns match well (Figure 2a inset). Taken together, ESI-MS indicates $Cd_1Au_{24}(SR)_{18}$ is neutral since the number of adducted Cs^+ ions equals the charge number. For $Hg_1Au_{24}(SR)_{18}$, the ESI spectrum (Figure 2b) showed peaks at m/z 3831.9 and 7531.0, assigned to $Hg_1Au_{24}(SR)_{18}Cs_2^{2+}$ (calcd m/z 3831.9) and $Hg_1Au_{24}(SR)_{18}Cs^+$ (calcd m/z 7530.8), confirmed by isotope pattern analysis (Figure 2b inset). Similar to the case of $Cd_1Au_{24}(SR)_{18}$, $Hg_1Au_{24}(SR)_{18}$ is also charge neutral. Considering the similar masses of Hg and Au, we note that the experimental isotope pattern and mass of $Hg_1Au_{24}(SR)_{18}$ differ from those of $Au_{25}(SR)_{18}$ (Figure 2b inset); hence, $Au_{25}(SR)_{18}$ as the product is ruled out. The charge neutrality of Hg- or Cd-doped alloy NCs is further confirmed by the absence of TOA^+ signals in the MALDI mass spectra (Figure S6) and NMR spectra (Figure S7).

The $Cd_1Au_{24}(SC_2H_4Ph)_{18}^0$ NCs obtained by the metal exchange method allow the growth of single crystals. X-ray crystallography determined the structure of the doped NCs (Figure 3, for details see SI). The $Cd_1Au_{24}^0$ cluster (ligand omitted for simplicity) adopts the same core–shell structure as that of Au_{25}^- and Au_{25}^0.[10] The $Cd_1Au_{24}^0$ core consists of a centered 13-atom icosahedral M_{13} core, further capped by a second shell comprised of 12 Au atoms. The structure of the

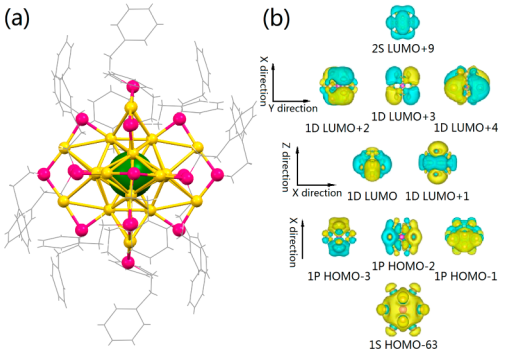

Figure 3. (a) Total structure of $Cd_1Au_{24}(PhC_2H_4S)_{18}^0$ NCs. Color labels: dark green = Cd; yellow = Au; magenta = S; all C and H atoms are shown in wireframe. (b) Superatomic orbital of $[Cd_1Au_{12}]^{6+}$.

DOI: 10.1021/ja511635g
J. Am. Chem. Soc. XXXX, XXX, XXX–XXX

Cd_1Au_{24} NC closely resembles Au_{25}^0, which has less distortion than Au_{25}^-.[10c] The distinct difference between these two NCs is the central atom in the M_{13} core, Cd in Cd_1Au_{24} NCs instead of Au. Hg is similar to Au in terms of the electronic structure, and it is not easy to distinguish Hg_1Au_{24} and Au_{25} NCs by X-ray crystallography. Hg_1Au_{24} should have the same structure as Cd_1Au_{24}, evidenced in our results by both having the same valence, the same NMR spectrum, and the loss of the same M_1Au_4 fragment in MALDI-MS.

To understand the bonding interactions between Cd and the $Au_{24}(SR)_{18}$ unit, deformation charge density analysis is carried out. The deformation charge density is defined as $\Delta\rho = \rho(Cd@Au_{24}(SR)_{18}) - \rho(Au_{24}(SR)_{18}) - \rho(Cd)$, which describes the bonding interactions between the central Cd atom and the surrounding $Au_{24}(SR)_{18}$ unit. The deformation charge density displayed in Figure S8 clearly shows the depletion of electronic charge density at the Cd atom, consistent with the Bader charge analysis (computational results and details are given in the SI). At the same time, the accumulation of electronic charge density is found in the space between the Cd atom and the Au_{12} shell, indicating relatively strong bonding interactions between the central Cd atom and the surrounding Au_{12} cage. On basis of the Bader charge analysis and the deformation charge density analysis, we propose that the central Cd atom is positively charged.

It is of interest to discuss whether $Cd_1Au_{24}(SR)_{18}$ is a superatomic species. $Cd_1Au_{24}(SR)_{18}$ has the same number of valence electrons as $Au_{25}(SR)_{18}^-$. According to the proposed electron counting rule for a superatom model,[9a] each staple motif of the thiolate-protected Au cluster can bind one electron of the inner metallic Au-core. In view of the structure of $Cd_1Au_{24}(SR)_{18}$, the central $Cd@Au_{12}$ core is protected by six dimeric staple motifs. Therefore, the $Cd@Au_{12}$ core can be considered as a $[Cd@Au_{12}]^{6+}$ species. The total number of valence electrons of $[Cd@Au_{12}]^{6+}$ is $8e^-$. Electronic structure analysis shows that the quasi-icosahedron $[Cd@Au_{12}]^{6+}$ possesses distinct delocalized 1S, 1P, 1D, and 2S superatom orbitals. As shown in Figure 3b, the 1S and three 1P orbitals are occupied. The 1D and 2S orbitals are all empty. The presence of delocalized superatomic orbitals in the $[Cd@Au_{12}]^{6+}$ core suggests that $Cd@Au_{24}(SR)_{18}$ falls into the category of superatomic cluster.

Detailed MALDI-MS analyses on $M_xAu_{25-x}(SR)_{18}$ offer more structural insight. The structure of $Au_{25}(SR)_{18}$ consists of a 13-atom core and six dimeric staples.[10] For Ag- and Cu-doped $M_xAu_{25-x}(SR)_{18}$, $M_xAu_{21-x}(SR)_{14}$ fragments were formed in both cases by losing a common $Au_4(SR)_4$ unit from the molecular ions (Figure S9a,b), consistent with the previous work on Cu- or Ag-doped $M_xAu_{25-x}(SR)_{18}$ NCs.[4] Loss of the $Au_4(SR)_4$ unit is associated with the surface $Au_2(SR)_3$ staples (i.e., the latter is detached from the Au_{13} core),[11a] and relevant works have been reported.[11b−d] According to the recently reported crystal structure of $Ag_xAu_{25-x}(SR)_{18}$, Ag atoms are at the surface of the 13-atom core,[12] indicating that Ag atoms only exchange with the Au atoms on the surface of the Au_{13} core. Unlike the cases of Ag- and Cu-doped NCs, both $Cd_1Au_{24}(SR)_{18}$ and $Hg_1Au_{24}(SR)_{18}$ NCs are missing a unit of $M_1Au_4(SR)_4$ (M = Cd/Hg) (Figure S9c,d), and some other fragmentation pathways were observed in the case of $Hg_1Au_4(SR)_4$ (Figure S9d).

X-ray photoelectron spectroscopy (XPS) measurements were carried out to confirm the presence of the doped metals in the NCs (Figure S10 for survey scans and Figure S11 for narrow scans). The Cu 2p peak (932.4 eV, Figure S11a) found in $Cu_xAu_{25-x}(SR)_{18}$ is close to that of pure Cu metal (932.6 eV) and the same as that of the Cu reduced by $Au_{25}(SR)_{18}^0$ NCs reported by Wu et al.[6a] The Ag 3d peak (368.30 and 374.30 eV, Figure S11b) of $Ag_xAu_{25-x}(SR)_{18}$ indicates that the incorporated Ag is neutral; i.e., the Ag^I complex was reduced by $Au_{25}(SR)_{18}^-$. In the case of $Cd_1Au_{24}(SR)_{18}$, the Cd signal (Cd 3d, 405.8 eV) was found (Figure S11c), but the binding energies of Cd^0 and Cd^{II} are not much different (404.9 vs 405.2 eV). The Hg 4f peak (101.2 eV, Figure S11d) of $Hg_1Au_{24}(SR)_{18}$ was observed.

The reactions between Au_{25} NCs and different metal complexes exhibit some interesting phenomena. The $Au_{25}(SR)_{18}^-$ reaction with $Cu^{II}(SR)_2$ was rapid, resulting in decomposition of Au_{25} NCs (Figure S12), and no Cu_xAu_{25-x} NCs could be found, but after addition of solid $NaBH_4$ to the reaction system, Cu_xAu_{25-x} NCs resulted (Figure S13). By extending the reaction time, more atoms of Cu could be doped into the Au_{25} NCs (Figure S13); the same is true for Ag doping. Of note, compared to the direct synthesis route for alloy NCs,[4d,e] the present metal exchange method leads to more Cu atoms doped into the cluster (Figure S13); for example, nine Cu atoms were doped into the NCs in ~24 h, while the direct synthesis of $Cu_xAu_{25-x}(SR)_{18}$ could only achieve a maximum five Cu atoms.[4d,e]

The resulting M_xAu_{25-x} NCs exhibit delocalized electron shell closing (DESC) at $8e^-$ (Scheme 1); this suggests that the superatom rules for pure Au NCs also apply for alloy NCs. [Note: The electron number is calculated as 25 − 18 − (−1) = 8 for $Ag_xAu_{25-x}(SR)_{18}^-$ and $Cu_xAu_{25-x}(SR)_{18}^-$, and 24 + 2 − 18−0 = 8 for $Cd_1Au_{24}(SR)_{18}^0$ and $Hg_1Au_{24}(SR)_{18}^0$, since Cu and Ag are of ns^1 configuration, whereas Hg and Cd are of ns^2.] The $8e^-$ requirement can explain our experimental observation: when there is no $NaBH_4$ in the reaction of Cu^{II} with $Au_{25}(SR)_{18}^-$, the product decomposes rapidly (Figure S12), because the exchange between Cu^{II} and Au atoms in the NC alters the total valence of Cu_1Au_{24} to 0 as the Au atom leaves the cluster in the form of Au^ISR, and its electronic number will become 25 − 18 − 0 = 7,

Scheme 1. Number of Delocalized Electrons (n_s) of Doped Nanoclusters

$Au_{25}(SR)_{18}^- + Ag(I)SR = Ag_xAu_{25-x}(SR)_{18}^-$	n_s=8 (stable)
$Au_{25}(SR)_{18}^- + Cu(II)SR = Cu_1Au_{24}(SR)_{18}^0$	n_s=7 (decomposed)
$Au_{25}(SR)_{18}^- + Cu(II)SR + NaBH_4 = Cu_xAu_{25-x}(SR)_{18}^-$	n_s=8 (stable)
$Au_{25}(SR)_{18}^- + Cd(II)SR = Cd_1Au_{24}(SR)_{18}^0$	n_s=8 (stable)
$Au_{25}(SR)_{18}^- + Hg(II)SR = Hg_1Au_{24}(SR)_{18}^0$	n_s=8 (stable)

Scheme 2. Metal Exchange Process of Nanoclusters Using Metal Complexes with the Metal Core Size Preserved[a]

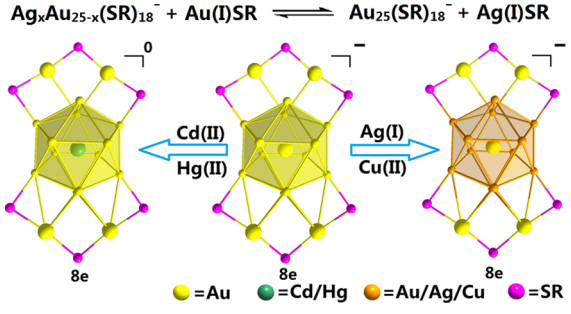

[a]Only part of the $Au_{25}(SR)_{18}$ structure is shown: the icosahedral Au_{13} core surrounded by two Au_2SR_3 motifs. The full structure of Au_{25} NCs is shown in Figure S15.[10] R = C_2H_4Ph. Note that $NaBH_4$ was needed in the reaction of Cu(II) with Au_{25} NCs.

DOI: 10.1021/ja511635g
J. Am. Chem. Soc. XXXX, XXX, XXX−XXX

hence destabilizing the resultant product. The DESC also explains why only one Cd or Hg atom could be doped into the Au_{25} NCs and why $Au_{25}(SR)_{18}^{0}$ could not react with Cd(II)/Hg(II) to form M_1Au_{24} NCs, because their valence and electronic numbers were changed. All of the obtained alloy NCs meet the $8e^-$ shell closing structure, suggesting that the metal exchange process in the NC regime is more critically dependent on the DESC and the 25-atom structural stability.

An important question arises naturally: What is the driving force of the metal exchange process? In the above results, the metals (in the thiolated complex form) that can be doped into the Au NCs all have fully filled d orbitals with $10e^-$. The d^{10}–d^{10} interaction is common in metals of groups 11 and 12. Thus, we hypothesize that the metal exchange may be caused in part by the d^{10}–d^{10} interaction between metal ions and Au NCs. This means that Ag^I can exchange for Au atoms in Au_{25} NCs, and the Ag atoms in the product (Ag_xAu_{25-x} NCs) may also be exchanged by Au^I ions. This is indeed what we observed experimentally (Figure S14). MALDI-MS spectra clearly show that the Ag atoms in Ag_xAu_{25-x} NCs were exchanged by Au^I gradually (Figure S14b,d). Furthermore, after addition of Ag^ISR, Ag atoms can be re-exchanged into the NCs. All these results indicate that the metal exchange is essentially reversible (Scheme 2).

Our results illustrate that, in the metal exchange process, the Au atoms in the $Au_{25}(SR)_{18}^-$ NC can be exchanged by metals with different activities (e.g., Cu, Ag, Cd, Hg, etc.) to produce new, stable NCs such as $Cd_1Au_{24}(SR)_{18}^{0}$ and $Hg_1Au_{24}(SR)_{18}^{0}$ in very high yields (~100%). This metal exchange method for alloy NCs is, to a large extent, associated with electron shell closing and the NC's structural stability, but less on the metal activity. These findings shed some new light on the metal exchange process at the atomic level, and this approach holds promise in future development as a versatile method for synthesizing alloy NCs that contain both high- and low-activity metal atoms with precise control of metal composition, doping site, and dopant number for specific applications. Future work will also elucidate how the Cd atom is doped into the center of the M_{13} core.

■ ASSOCIATED CONTENT

Supporting Information

Experimental details and characterization data. This material is available free of charge via the Internet at http://pubs.acs.org.

■ AUTHOR INFORMATION

Corresponding Author

*zmz@ahu.edu.cn

Author Contributions

§S.W. and Y.S. contributed equally.

Notes

The authors declare no competing financial interest.

■ ACKNOWLEDGMENTS

We acknowledge financial support by the NSFC (21072001, 21201005, 21372006), the Ministry of Education and Ministry of Human Resources and Social Security, the Education Department of Anhui Province, the Anhui Province International Scientific and Technological Cooperation Project, and the 211 Project of Anhui University. Y.P. acknowledges financial support by NSFC (21373176, 21422305).

■ REFERENCES

(1) (a) Negishi, Y.; Kurashige, W.; Niihori, Y.; Nobusada, K. *Phys. Chem. Chem. Phys.* **2013**, *15*, 18736. (b) Jin, R.; Nobusada, K. *Nano Res.* **2014**, *7*, 285.

(2) (a) Xie, S.; Tsunoyama, H.; Kurashige, W.; Negishi, Y.; Tsukuda, T. *ACS Catal.* **2012**, *2*, 1519. (b) Qian, H.; Jiang, D.; Li, G.; Gayathri, C.; Das, A.; Gil, R. R.; Jin, R. *J. Am. Chem. Soc.* **2012**, *134*, 16159.

(3) (a) Wang, Q.; Lee, Y.; Crespo, O.; Deaton, J.; Tang, C.; Gysling, H. J.; Gimeno, C.; Larraz, C.; Villacampa, M. D.; Laguna, A.; Eisenberg, R. *J. Am. Chem. Soc.* **2004**, *126*, 9488. (b) Jia, J.; Wang, Q. *J. Am. Chem. Soc.* **2009**, *131*, 16634. (c) Udayabhaskararao, T.; Sun, Y.; Goswami, N.; Pal, S. K.; Balasubramanian, K.; Pradeep, T. *Angew. Chem., Int. Ed.* **2012**, *51*, 2155. (d) Pei, X.; Yang, Y.; Lei, Z.; Wang, Q. *J. Am. Chem. Soc.* **2013**, *52*, 6435. (e) Wang, S.; Meng, X.; Das, A.; Li, T.; Song, Y.; Cao, T.; Zhu, X.; Zhu, M.; Jin, R. *Angew. Chem., Int. Ed.* **2014**, *53*, 2376.

(4) (a) Negishi, Y.; Kurashige, W.; Niihori, Y.; Iwasa, T.; Nobusada, K. *Phys. Chem. Chem. Phys.* **2010**, *12*, 6219. (b) Negishi, Y.; Iwai, T.; Ide, M. *Chem. Commun.* **2010**, *46*, 4713. (c) Qian, H.; Barry, E.; Zhu, Y.; Jin, R. *Acta Phys. Chim. Sin.* **2011**, *27*, 513. (d) Negishi, Y.; Munakata, K.; Ohgake, W.; Nobusada, K. *J. Phys. Chem. Lett.* **2012**, *3*, 2209. (e) Gottlieb, E.; Qian, H.; Jin, R. *Chem.—Eur. J.* **2013**, *19*, 4238. (f) Kurashige, W.; Munakata, K.; Nobusada, K.; Negishi, Y. *Chem. Commun.* **2013**, *49*, 5447.

(5) (a) Kumara, C.; Dass, A. *Nanoscale* **2011**, *3*, 3064. (b) Kumara, C.; Dass, A. *Nanoscale* **2012**, *4*, 4084. (c) Negishi, Y.; Igarashi, K.; Munakata, K.; Ohgake, W.; Nobusada, K. *Chem. Commun.* **2012**, *48*, 660. (d) Kothalawala, N.; Kumara, C.; Ferrando, R.; Dass, A. *Chem. Commun.* **2013**, *49*, 10850. (e) Yang, H.; Wang, Y.; Lei, J.; Shi, L.; Wu, X.; Mäkinen, V.; Lin, S.; Tang, Z.; He, J.; Häkkinen, H.; Zheng, L.; Zheng, N. *J. Am. Chem. Soc.* **2013**, *135*, 9568. (f) Yang, H. Y.; Wang, Y.; Huang, H. Q.; Gell, L.; Lehtovaara, L.; Malola, S.; Häkkinen, H.; Zheng, N. F. *Nat. Commun.* **2013**, *4*, 2422. (g) Yang, H.; Wang, Y.; Yan, J.; Chen, X.; Zhang, X.; Häkkinen, H.; Zheng, N. F. *J. Am. Chem. Soc.* **2014**, *136*, 7197. (h) Puls, A.; Jerabek, P.; Kurashige, W.; Förster, M.; Molon, M.; Bollermann, T.; Winter, M.; Gemel, C.; Negishi, Y.; Frenking, G.; Fischer, R. A. *Angew. Chem., Int. Ed.* **2014**, *53*, 4327. (i) Ganesamoorthy, C.; Weßing, M. S. J.; Kroll, M. S. C.; Seidel, R. W.; Gemel, C.; Fischer, R. A. *Angew. Chem., Int. Ed.* **2014**, *53*, 8077.

(6) (a) Wu, Z. *Angew. Chem., Int. Ed.* **2012**, *51*, 2934. (b) Li, H.; Yue, Y.; Liu, T.; Li, D.; Wu, Y. *J. Phys. Chem. C* **2013**, *117*, 16159. (c) Sun, J.; Wu, H.; Jin, Y. *Nanoscale* **2014**, *6*, 5449. (d) Wang, S.; Meng, X.; Feng, Y.; Sheng, H.; Zhu, M. *RSC Adv.* **2014**, *4*, 9680.

(7) Reveles, J. U.; Claybome, P. A.; Reber, A. C.; Khanna, S. N.; Pradhan, K.; Sen, P.; Pederson, R. *Nat. Chem.* **2009**, *1*, 310.

(8) Walter, M.; Moseler, M. *J. Phys. Chem. C* **2009**, *113*, 15834.

(9) (a) Walter, M.; Akola, J.; Lopez-Acevedo, O.; Jadzinsky, P. D.; Calero, G.; Ackerson, C. J.; Whetten, R. L.; Grönbeck, H.; Häkkinen, H. *Proc. Natl. Acad. Sci. U.S.A.* **2008**, *105*, 9157. (b) Häkkinen, H. *Chem. Soc. Rev.* **2008**, *37*, 1847. (c) Jiang, D.-e.; Dai, S. *Inorg. Chem.* **2009**, *48*, 2720. (d) Aikens, C. M. *J. Phys. Chem. Lett.* **2011**, *2*, 99.

(10) (a) Heaven, M. W.; Dass, A.; White, P. S.; Holt, K. M.; Murray, R. W. *J. Am. Chem. Soc.* **2008**, *130*, 3754. (b) Zhu, M.; Aikens, C. M.; Hollander, F. J.; Schatz, G. C.; Jin, R. *J. Am. Chem. Soc.* **2008**, *130*, 5883. (c) Zhu, M.; Eckenhoff, W. T.; Pintauer, T.; Jin, R. *J. Phys. Chem. C* **2008**, *112*, 14221.

(11) (a) Wu, Z.; Gayathri, C.; Gil, R. R.; Jin, R. *J. Am. Chem. Soc.* **2009**, *131*, 6535. (b) Jiang, D.; Walter, M.; Dai, S. *Chem.—Eur. J.* **2010**, *16*, 4999. (c) Macdonald, M.; Cheverie, D.; Zhang, P.; Qian, H.; Jin, R. *J. Phys. Chem. C* **2011**, *115*, 15282. (d) Krishna, K. S.; He, M.; Bruce, D. A.; Kumar, C. S. S. R. *Nanotechnol. Rev.* **2014**, *3*, 311.

(12) Kumara, C.; Aikens, C. M.; Dass, A. *J. Phys. Chem. Lett.* **2014**, *5*, 461.

DOI: 10.1021/ja511635g
J. Am. Chem. Soc. XXXX, XXX, XXX–XXX